

CHAPTER V

MECHANICAL AND THERMAL PROPERTIES OF POLYPROPYLENE NANOCOMPOSITE FILMS

5.1 Abstract

Effect of copper nanoparticles (CuNP) content (5, 10, 15 and 20 wt% of total nanoparticles) on clarity, mechanical properties and thermal properties (DSC and TGA) of polypropylene (PP) nanocomposite blown film was investigated. PP nanocomposite films were fabricated via water-quenched blown film extrusion. Sodium neutralized ethylene-methacrylic acid ionomer (Surlyn) of 2 phr was used to modify compatibility between PP and nanoparticles. With the presence of CuNPs, PP nanocomposite blown films were haze and had higher yellowish tinge. Even having 1 wt% of nanoparticles in films, these water-quenched blown films showed elongation at break in machine direction over 300%. Adding PVP-coated CuNPs into PP films showed positive effect on tensile strength of nanocomposite films. This is due to Surlyn ionomer and nanoparticles acted as nucleating sites to increase crystallinity of PP nanocomposite films. Thermal stability of PP nanocomposite films was improved with the presence of nanoparticles. From the overall mechanical properties and clarity, it indicates that the PP nanocomposite films would be capable to be used in prepacked chilled fish packaging.

5.2 Introduction

Polypropylene is a versatile thermoplastic polymer from the monomer propylene. It can be fabricated into packaging film that has good clarity, resistance to UV light, excellent chemical and abrasion resistance. Although polypropylene (PP) film has widely used for food packaging, but it does not have oxygen and moisture barrier properties. This limits using polypropylene film in some fresh food packaging since it is not breathable. Adding micro perforation (a series of tiny holes punched in plastic film) into PP film is performed in order to use for biochemically active agricultural products such as fresh fruits, fresh vegetables, fresh herbs, and flowers,

and more particularly for use in modifying the flow of oxygen and carbon dioxide into and/out of a fresh produce container.

Over the last few decades, a great amount of effort has been devoted to fabrication of polymer layered silicate nanocomposites because of their exceptionally improved mechanical properties, such as improved stiffness, barrier properties, and flame-retardance at low filler loading (3-5 wt%). Among the nanocomposites based on various polymers, polypropylene-clay nanocomposites have attracted special attention due to their commercial importance. However, due to the low polarity of PP, it is difficult to get the exfoliated and homogeneous dispersion of the silicate layer at the nanometer level in the polymer. This is mainly due to the fact that the silicate clays layers have polar hydroxyl groups and are compatible only with polymers containing polar functional groups. When preparing nanocomposites by melt compounding, shear alone is not enough to provide nanometric dispersion of clay platelets.

As a class of ionomer, Surlyn developed by Dupont is ethyleneco-methacrylic acid (E-MAA) polymer, in which a small amount of methyl-carboxylic acid is partially neutralized by metal bases, e.g., Na^+ , Li^+ and Zn^{2+} . Here, the associated ionic groups form ion-rich domains in the nanometer size (ionic aggregates/cluster) in the hydrophobic polyethylene (PE) matrix. The presence of these aggregates deeply influences mechanical and melt-flow properties of the resulting materials. The general molecular structure of Surlyn is as follows:

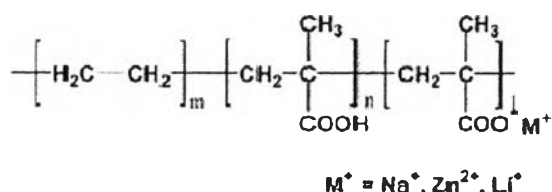


Figure 5.1 Surlyn structure (Lim *et al.*, 2010).

where m , n , and l are the segment number of units. The presence of the pendant ionic groups in the ionomer creates favorable interaction between ionomer and

aluminosilicate clay. Lim *et al.* (2010) reported that the addition of ionomer significantly enhanced the dispersion of clays. Apart from the localization inside the dispersed Surlyn domain, clay platelets were also localized at the interface between PP and Surlyn, as evidenced by SEM pictures. The viscoelastic properties of the PP/Surlyn/OMMT ternary hybrids exhibited a remarkable increase upon the addition of the ionomer, which could be attributed to the increased exfoliation of clays and interfacial contribution caused by silicate layers at the interface.

There have been a few reports fabricated polyolefin-clay nanocomposite by blown film extrusion and studied the properties of blown films. Zhong *et al.* (2005, 2007) compounded ethylene vinyl acetate (EVA), low density polyethylene (LDPE), and high density polyethylene (HDPE) with an organically modified montmorillonite with melt compounding and blown into films. The morphology studies showed that all three types of film involve intercalated clay particles. The tensile testing data showed that the clay enhancing effects apply mainly to the modulus, instead of to the strength. It was found that the clay enhancing effects are function of the matrix. The mechanical and oxygen barrier properties of clay/EVA systems increased with clay loading. Both the tensile modulus and oxygen barrier of EVA doubled at 5 wt% clay. Maleic anhydride grafted polyethylene (MAPE) usually was used as a compatibilizer for LDPE and HDPE-based nanocomposites. However, the MAPEs were found to weaken the oxygen barrier of the PEs, especially for HDPE. They discussed that this was a result of less compactness caused by the large side groups and the increase in polarity of the MAPEs. Incorporating clay 5 wt% improves the oxygen barrier by 30% and the tensile modulus by 37% for the LDPE/MAPE system. Incorporation of clay does not enhance the properties of the HDPE-based systems, likely due to large domain structure and poor bonding.

The objective of the research was to develop active packaging film made of polypropylene based on nanotechnology. Bentonite organoclay and copper nanoparticles were chosen to add into polypropylene films for barrier property and antimicrobial activity. Copper nanoparticles were synthesized via a chemical method in aqueous solution using ascorbic acid to be a reducing agent and polyvinylpyrrolidone as a dispersant in our laboratory. Fabrication of nanocomposite films was performed via a water-cooled blown film extrusion which was

conventional used to produce clear films for food packaging in Thailand. Ethylene-methacrylic acid ionomer (Surlyn[®]) was used to improve exfoliation of clay platelets. In this chapter, effect of CuNP content (5, 10, 15 and 20 wt% of total particles) on clarity, mechanical and thermal properties of polypropylene nanocomposite film were investigated. XRD was used to investigate the exfoliation of Bentonite organoclay in the blown film samples, and SEM was used to study the compatibility of the PP/Surlyn/OBEN-CuNP tertiary phases.

5.3 Experimental

5.3.1 Materials

Polypropylene homopolymer (PP 1102K) pellets with MFI of 4 g/10 min (190 °C, 2.16 kg) was purchased from IRPC Co. Ltd., Thailand. Additives such as slip and antiblock agents were not added. Surlyn[®]P350, sodium neutralized ethylene-methacrylic acid ionomer, with MFI of 4.5 g/10min (190 °C, 2.16 kg) was purchased from Dupont[™], USA. Bentonite organoclay (OBEN) was prepared in our laboratory by using sodium activated Bentonite (kindly supplied by Thai Nippon Co., Ltd., Thailand) and distearoylethyl hydroxyethylmonium methosulfate and cetearyl alcohol. Copper nanoparticles were synthesized previously in the laboratory following the procedure described in Wu *et al.* (2006).

5.3.2 Preparation of OBEN/CuNP Masterbatch

The masterbatch of OBEN/CuNP was prepared by mixing dried OBEN/CuNP mixture with Surlyn[®] P350 in a ratio of 1:2 by weight, in a Haake Rheomex PTW-16 co-rotating twin-screw extruder with $D = 16$ mm and $L/D = 25$. The operating temperature of extruder was set at 180 °C with a screw speed of 70 rpm. Extrudate was pelletized for further mixed with PP pellets in a ratio of PP:OBEN/CuNP_x = 99:1 wt%. The letter x refers to copper nanoparticle content in wt% adding into OBEN-CuNP mixture.

5.3.3 Preparation of Neat PP and PP Nanocomposite Films

Neat PP, PP/Surlyn, PP/OBEN, and PP/OBEN-CuNP_x film samples were fabricated using a water-quenched blown film extruder (PP50, Thailand). Temperature profiles were 210, 220, 220, and 210 °C from feed zone to die. Screw

speed was kept constant at 80 rpm. Bubble forming ring of 23 cm in water bath was used, which final width of blown film was about 22-23 cm. Nip-roll speed and pull-out speed were adjusted to produce blown films with final thickness of 40-50 μm . Table 5.1 summaries the abbreviations of the blown film samples and their compositions after mixing the masterbatch with neat PP.

Table 5.1 Abbreviations and composition of blown films

Abbreviations	PP (wt%)	Bentonite organoclay (wt%)	CuNP (wt%)	Surlyn (phr)
Neat PP	100.0	-	-	-
PP/Surlyn	100.0	-	-	2
PP/OBEN	99.0	1.00	-	2
PP/OBEN-Cu5	99.0	0.95	0.05	2
PP/OBEN-Cu10	99.0	0.90	0.10	2
PP/OBEN-Cu15	99.0	0.85	0.15	2
PP/OBEN-Cu20	99.0	0.80	0.20	2

5.3.4 Clarity and Mechanical Properties of Neat PP and PP Nanocomposite Films

Clarity and color of film samples was determined using a UV-VIS-NIR spectrophotometer (Perkin Elmer Lambda 900) in transmittance mode. Lightness (L^*) and color in Lab system was reported.

Tensile strength and elongation at break of neat PP and PP nanocomposite films were measured in accordance to ASTM D-882 using a universal testing machine (Instron 5969, Instron Engineering Corp., USA). Using a sharp razor blade, film specimens were cut from blown films in machine and transverse directions to obtain rectangular strips of 25.4 mm x 127 mm long. Gauge length of 50 mm was used, and test speed was set at 50 mm/min. Before testing, thickness of film specimens was measured along the length in 5 different areas to

determine average thickness. Ten specimens in machine and transverse directions were tested, and five data with closed standard deviation was selected to represent the average and standard deviation.

Tear propagation resistance of neat PP and PP nanocomposite films were measured in accordance to ASTM D-1938 using a universal testing machine (Instron 5969, Instron Engineering Corp., USA). Using a sharp razor blade, film specimens were cut from blown films in machine and transverse directions to obtain rectangular strips of 25 mm x 76 mm long. Before testing, thickness of film specimens was measured along the length in 5 different areas to determine average thickness. The grip-separation speed was set at 250 mm/min. The load necessary to propagate the tear through the entire unslit 25 mm portion was recorded. Ten specimens in machine and transverse directions were tested, and five data with closed standard deviation was selected to represent the average and standard deviation.

5.3.5 Morphology of Neat PP and PP Nanocomposite Films

Dispersion of nanoparticles (OBEN and OBEN-CuNP) in PP matrix and compatibility of the PP/Surlyn/OBEN-CuNP tertiary phases were carried out using SEM (JEOL/JEM 5800 LV). Film samples were dipped and fractured in liquid nitrogen. Then the samples were sputtered with gold before viewing under scanning electron microscope (SEM) operating.

Nanoscale dispersion of nanoparticles (OBEN and OBEN-CuNP) in PP matrix was studied using XRD (Bruker AXS Model D8) diffractometer with CuK_α radiation operate at 40 kV and 30 mA. The film samples were observed on the 2θ range of 2-20 degree with a scan speed of 2 degree/min and scan step of 0.01 degree.

5.3.6 Thermal Properties of Neat PP and PP Nanocomposite Film

Crystallinity and melting behaviors of neat PP and PP nanocomposite films were studied with a Differential Scanning Calorimeter (Mettler DSC 1, Mettler Toledo, Switzerland). All operations were performed under a nitrogen atmosphere. The samples were first heated from 25 °C to 250 °C at the heating rate of 10 °C/min in order to eliminate the influence of thermal history and then cooled down at rate of

10 °C/min from 250 °C to 25 °C to observe the melt crystallization behavior. The samples were then reheated to 250 °C at the same rate.

Thermogravimetric analysis (TGA) was used to study thermal stability of neat PP and PP nanocomposite films. TG-DTA curves were collected on a METTLER TG/DTA instrument. The degradation temperature, initial degradation temperature, weight loss and final degradation temperature of the samples were determined. The samples were loaded on ceramic pan and heated from 25 °C to 800 °C at heating rate 10 °C/min and flow under nitrogen gas of 200 ml/min.

5.4 Results and Discussion

5.4.1 Clarity and Color of Neat PP and PP Nanocomposite Films

Since the film samples were produced via water-quenched blown film extrusion, high transparent films were produced. By naked eyes, it is seen that PP/OBEN blown films were clear films similarly to neat PP films, however, it was yellowish tinge from dispersion of Bentonite organoclay in PP matrix. This could be attributed to the good organoclay dispersion achieved in these nanocomposite films resulting from the use of Surlyn and optimum processing conditions. PP nanocomposite films with CuNP were haze and had yellowish tinge as presented in Fig.5.2. Neat PP and PP/Surlyn films had a smooth texture, while PP nanocomposite films had rougher texture due to the presence of inorganic particles. However, all of the films produced, including those with the nanoparticles, contained very few visual imperfections such as gels or fisheyes.

Fig.5.3 and Fig.5.4 show L^* (lightness) and b^* (yellowness) of neat PP and PP nanocomposite blown films, respectively. All sample films were translucent film with L^* over 95. Yellowness of film samples results from dispersion of OBEN and copper nanoparticles in PP matrix. From b^* value, it indicates that yellowness of PP nanocomposite films were increased with respect to CuNP content.

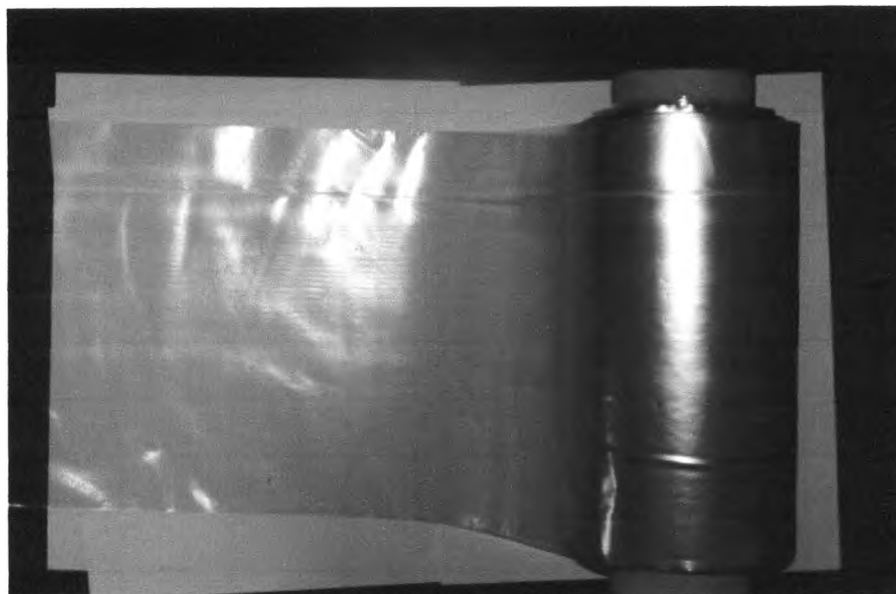


Figure 5.1 Appearance of PP nanocomposite blown films adding OBEN/CuNP-5.

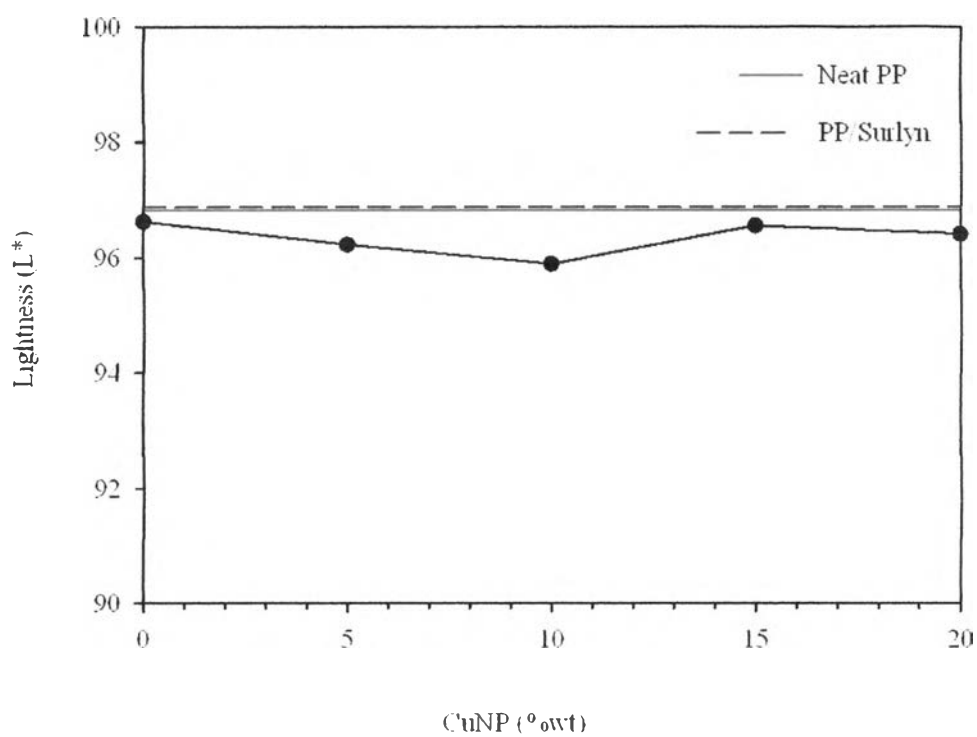


Figure 5.2 Lightness (L*) of neat PP and PP nanocomposite blown films.

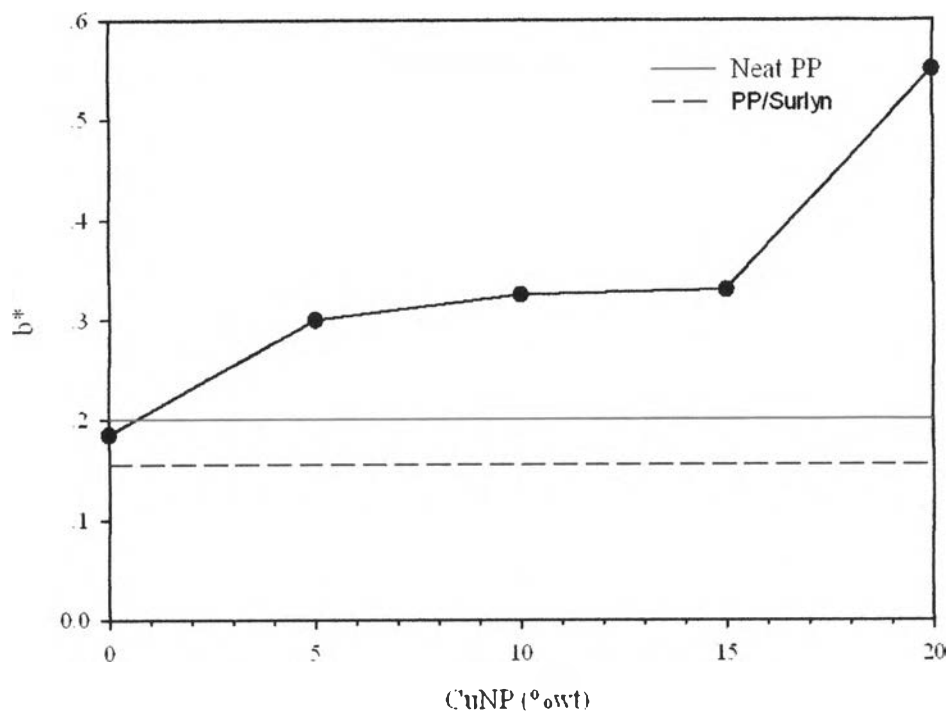


Figure 5.1 b^* of neat PP and PP nanocomposite blown films. Value of b^* indicates yellowness of films.

5.4.2 Mechanical Properties of Neat PP and PP Nanocomposite Films

Tensile tests were performed on neat PP, PP/Surllyn and PP nanocomposite blown films to investigate influence of CuNP content on mechanical properties of the blown film samples. Fig.5.5 shows tensile strength (at break) of neat PP, PP/Surllyn and PP nanocomposite blown films in machine and transverse direction. Generally, the tensile strength in transverse direction of water-quenched blown films is somewhat lower than those in machine direction because of limitation of bubble extension (less stresses) in transverse direction from fixed ring in the water bath to allow molecular orientation of polymer molecules.

Also, the representative stress-strain curve of the blown films is presented in Fig.5.6. The stress-strain curve of neat PP blown films is characterized by an initial high slope, followed by a plateau with gradually increasing stress until fracture. Macroscopically, the neat PP films were stretched uniformly up to fracture. PP exhibits a typical cold-drawn behavior. It experiences yield, stress whitening,

cold-drawing, followed by the final break during a tension excursion. During cold-drawing, chains unfold and then align in the stress direction, which this reorganization produces a much longer, thinner, and stronger film (Zhong *et al.*, 2007). Deformation of the PP/Surllyn blend films was macroscopically uniform, but stress-whitening was faint similarly to the stress-strain curve of PP/PE blend reported in Chang *et al.* (2002). Lim *et al.* (2010) reported the deterioration of tensile strength for PP/Surllyn 95/5 wt% blend compared to the neat PP. They denoted the decrease in tensile strength resulted from low interfacial adhesion between the phases which debonding between PP matrix and Surllyn dispersed phases was observed in the cryo-fractured SEM micrographs. The reduction of tensile strength of PP/Surllyn is about 14% compared to the tensile strength of neat PP films.

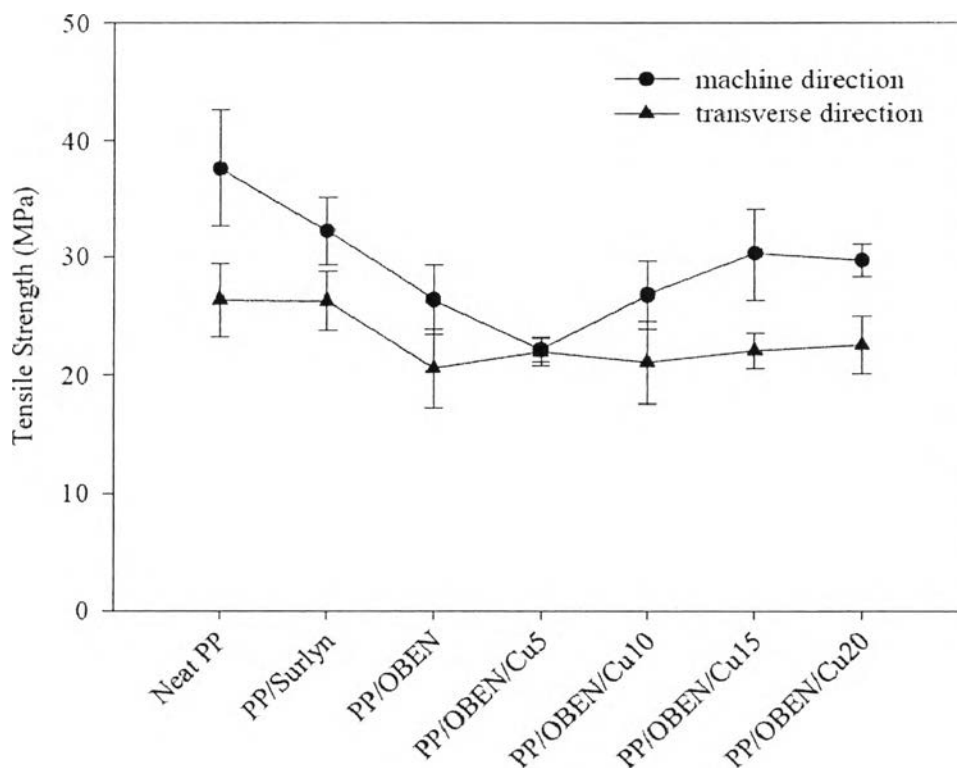


Figure 5.5 Tensile strength of neat PP and PP nanocomposite blown films.

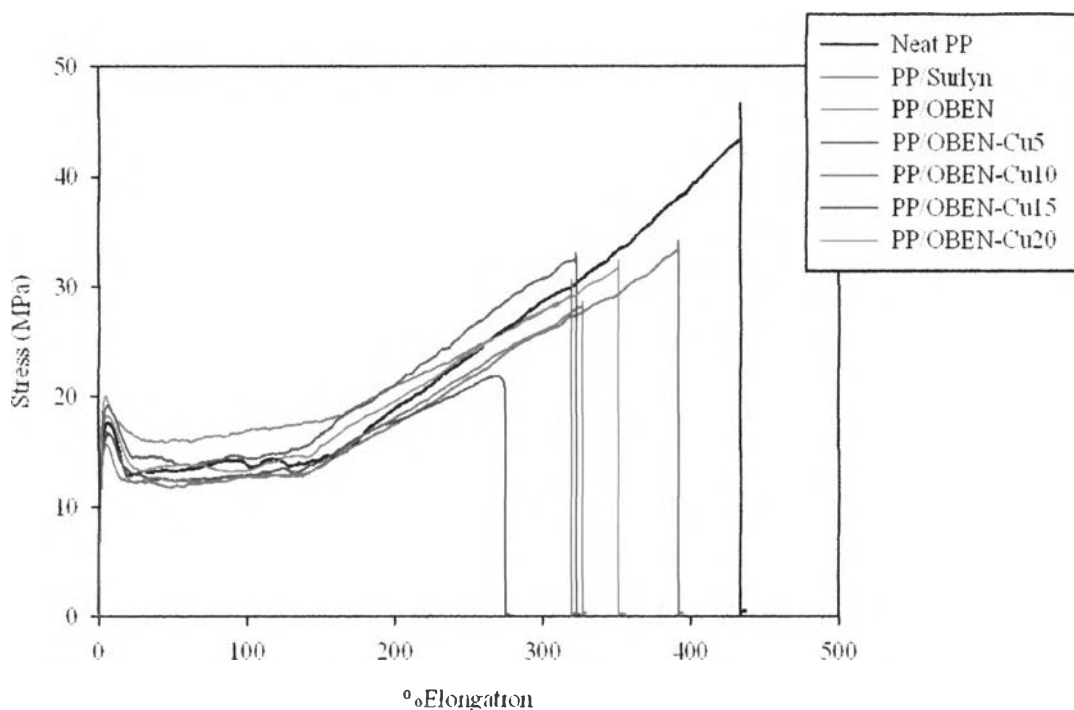


Figure 5.1 The stress-strain curves of neat PP and PP nanocomposite blown films cutting along the machine direction (MD).

Adding 1 wt% Bentonite organoclay further decreased tensile strength (at break) of PP nanocomposite blown film. Zhong *et al.* (2007) explained the strength deterioration of 2 wt% clay/LDPE films compared to neat LDPE films relating to the fact that clay tactoids hinder the orientation of polyethylene lamellae during cold drawing. From SEM micrographs, good dispersion of OBEN-Surlyn masterbatch in PP matrix is observed, however, voids around some dispersed phases are evident indicating poor adhesion between PP and OBEN-Surlyn. These would become stress concentration during the extension of blown films and reduced the cold-drawing phenomenon of PP molecules.

Adding PVP-coated CuNP into PP matrix shows positive effect on tensile strength in machine direction of nanocomposite blown films, except with the lowest content of 5 wt% CuNP. Since the amount of nanoparticles was kept constant of 1 wt% of nanocomposite films, adding higher content of denser CuNP decreased the volume of OBEN nanoclay, therefore, the better dispersion of nanoclay into

Surlyn dispersed phases was achieved. As a result, the ability of the dispersed ionomer particles to form cavitation under uniaxial tensile stress is decreased (Lim *et al.*, 2010), resulting to the decrease in elongation at break and higher stress is needed to extend the films. For the lowest tensile in PP/OBEN-CuNP5 films, it is attributed to there are more voids due to debonding of nanoparticles from PP matrix compared to other nanocomposite film samples as evident in SEM micrographs.

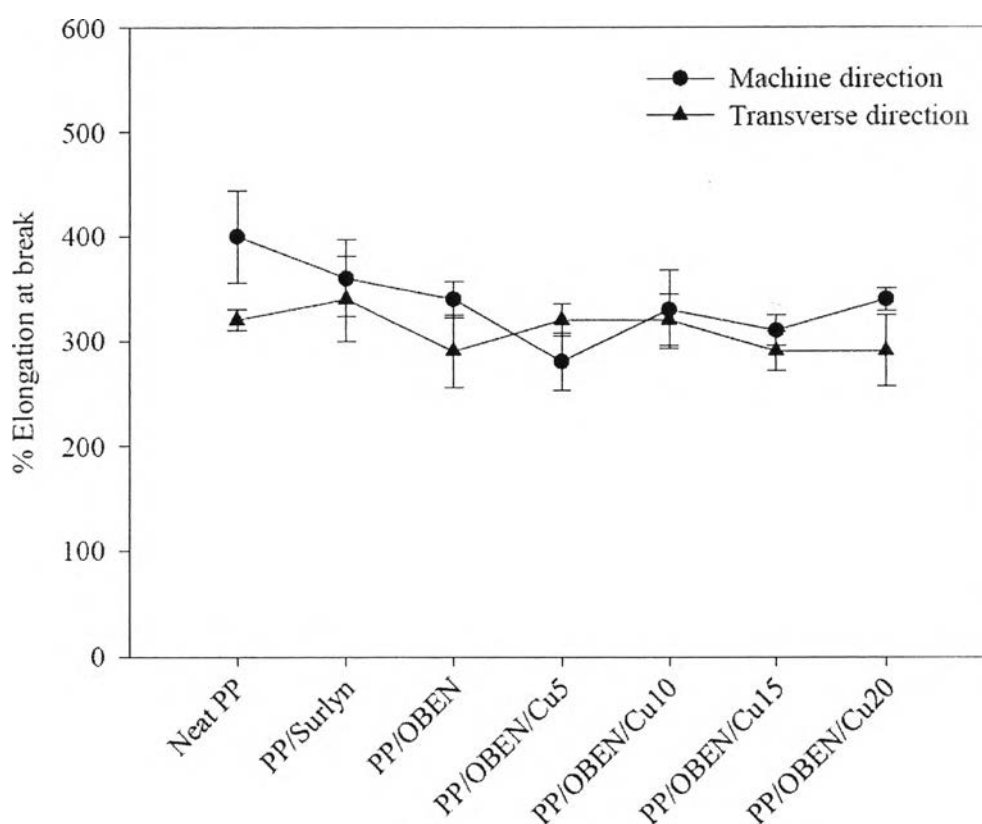


Figure 5.7 Percentage of elongation at break of neat PP and PP nanocomposite blown films.

Fig.5.7 shows the percentage of elongation at break of neat PP, PP/Surlyn and PP nanocomposite blown films in machine and transverse direction. The elongation at break is very sensitive to the strength of the interface, and it is used to evaluate the efficiency of compatibility. It is seen that % elongation at break of PP/Surlyn and PP/OBEN films were lower than those of neat PP film, indicating the

insufficient interfacial bonding between Surlyn and PP matrix to prevent debonding of Surlyn dispersed phases from PP matrix. Compared to PP/OBEN films, incorporating CuNP into OBEN did not affect % elongation at break in machine direction significantly, except films with 5 wt% CuNP. The decrease of elongation at break in PP/OBEN-Cu5 film indicates there were more inhomogeneous regions to initiate premature breakage. From SEM micrographs, the PP/OBEN-Cu5 cross-section surfaces shows more voids due to debonding of nanoparticles from PP matrix during the cryo-fracture compared to other samples.

In contrast, % elongation at break in transverse direction of nanocomposite films decreased with respect to CuNP content. This resulted from water-quenched process that bubbles were quenched via open-ring in the water bath. While the bubble was quenched to not be able to expand in transverse direction, the nip-roll pulled blown films to stretch along the machine direction resulting on yielding of PP matrix around the agglomeration of particles while orienting Surlyn dispersed phases along the machine direction. The combination of these phenomena weakened quenched blown films in the transverse direction as seen in the results. Tensile results are summarized in Table 5.2.

Table 5.2 Tensile properties of neat PP and PP nanocomposite blown films

Abbreviations	Tensile strength (MPa)		% Elongation at break	
	MD	TD	MD	TD
Neat PP	37.6 ± 4.95	26.4 ± 3.08	400 ± 44.27	320 ± 10.29
PP/Surlyn	32.2 ± 2.91	26.3 ± 2.43	360 ± 37.01	340 ± 40.60
PP/OBEN	26.4 ± 2.89	20.6 ± 3.36	340 ± 17.60	290 ± 34.48
PP/OBEN-Cu5	22.2 ± 1.05	22.0 ± 1.17	280 ± 27.02	320 ± 15.67
PP/OBEN-Cu10	26.8 ± 2.88	21.1 ± 3.48	330 ± 37.27	320 ± 24.86
PP/OBEN-Cu15	30.3 ± 3.85	22.1 ± 1.55	310 ± 14.39	290 ± 19.03
PP/OBEN-Cu20	29.7 ± 1.35	22.6 ± 2.45	340 ± 10.91	290 ± 34.15

Since PP is high extension plastics, tear strength at maximum loading is reported in this study. Fig.5.8 shows tear strength at maximum loading of neat PP, PP/Surlyn and PP nanocomposite blown films in machine and transverse direction. In contrast to tensile results, for all film samples, the tear strength or resistance to tear propagation is higher along the transverse direction relative to machine direction. This results from high orientation of polymer molecules in machine direction during the water-quenched blown film process as discussed in tensile test. It is seen that tear strength in transverse direction of PP nanocomposite films with were in the same range of neat PP films except the one with CuNP content of 10 wt%, while tear strength in machine direction of nanocomposite films increased with respect to CuNP content similarly to tensile test. This comes from the fact that high extension PP films were torn and stretched during the tear propagation test, which resembled the action in the tensile test. The lowest tear strength in PP/OBEN-Cu10 films comes from the large Surlyn/OBEN dispersed phases as seen in SEM micrograph. This behaves as stress concentration to allow breakage of films to occur around the surface easier than the smaller ones.

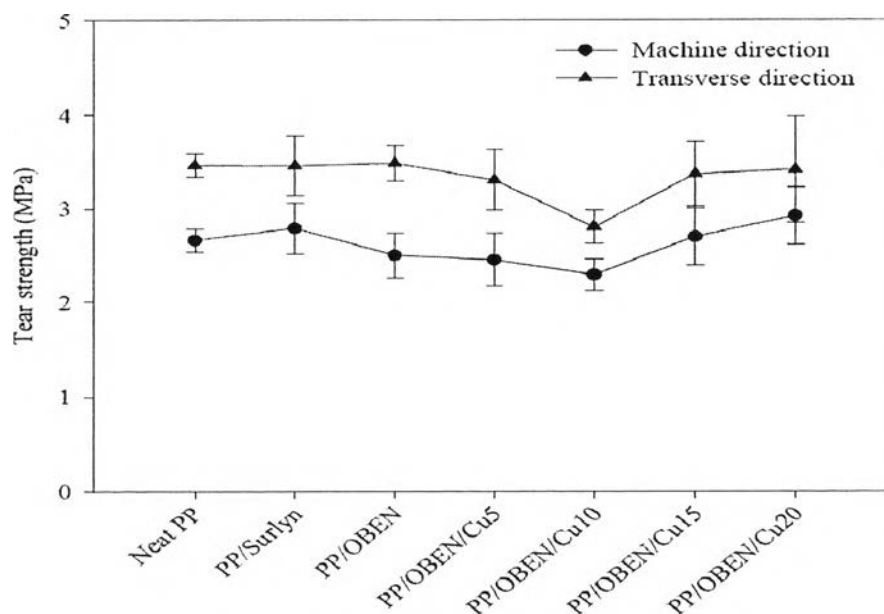


Figure 5.8 Tear strength at maximum loading of neat PP and PP nanocomposite films.

5.4.3 Morphology of Neat PP and PP Nanocomposite Films

Fig.5.9 and Fig.5.10 show SEM micrographs of cryo-fractured cross-section surfaces of neat PP, PP/Surlyn, PP/Surlyn/OBEN, and PP/Surlyn/OBEN-CuNP_x blown films. Compared to neat PP, it is clearly observed that there are many smooth particles dispersed in PP matrix indicating immiscibility between PP and Surlyn ionomer. Debonding of ionomer aggregates from PP matrix during the cryo-fracture is observed implying low adhesion between them. It should be noted that the elongated Surlyn phases are results from the cryo-fracture since Surlyn is rubber-like even at the low temperature.

In PP/Surlyn/OBEN, larger dispersed phases are observed which results from relatively stiffer Surlyn/OBEN dispersed phases to be sheared and dispersed into PP matrix during the blown film extrusion. There are some of silicate layers localized at the phase boundary between PP and Surlyn similarly to Lim's report (2010). In PP/Surlyn/OBEN-Cu5 sample, debonding of Surlyn dispersed phases are evident implying poor interfacial adhesion between the phases. In PP/Surlyn/OBEN-Cu10, some larger dispersed phases are present indicating to less dispersion of OBEN/Surlyn. However, the dispersed phases become smaller closed to the PP/OBEN when the CuNP content is 15 and 20 wt%. The change in size of dispersed phase is attributed to the lower volume of nanoclay dispersed the Surlyn, so that the Surlyn/OBEN is more flexible to be sheared and broken into smaller spheres during the blown film extrusion.

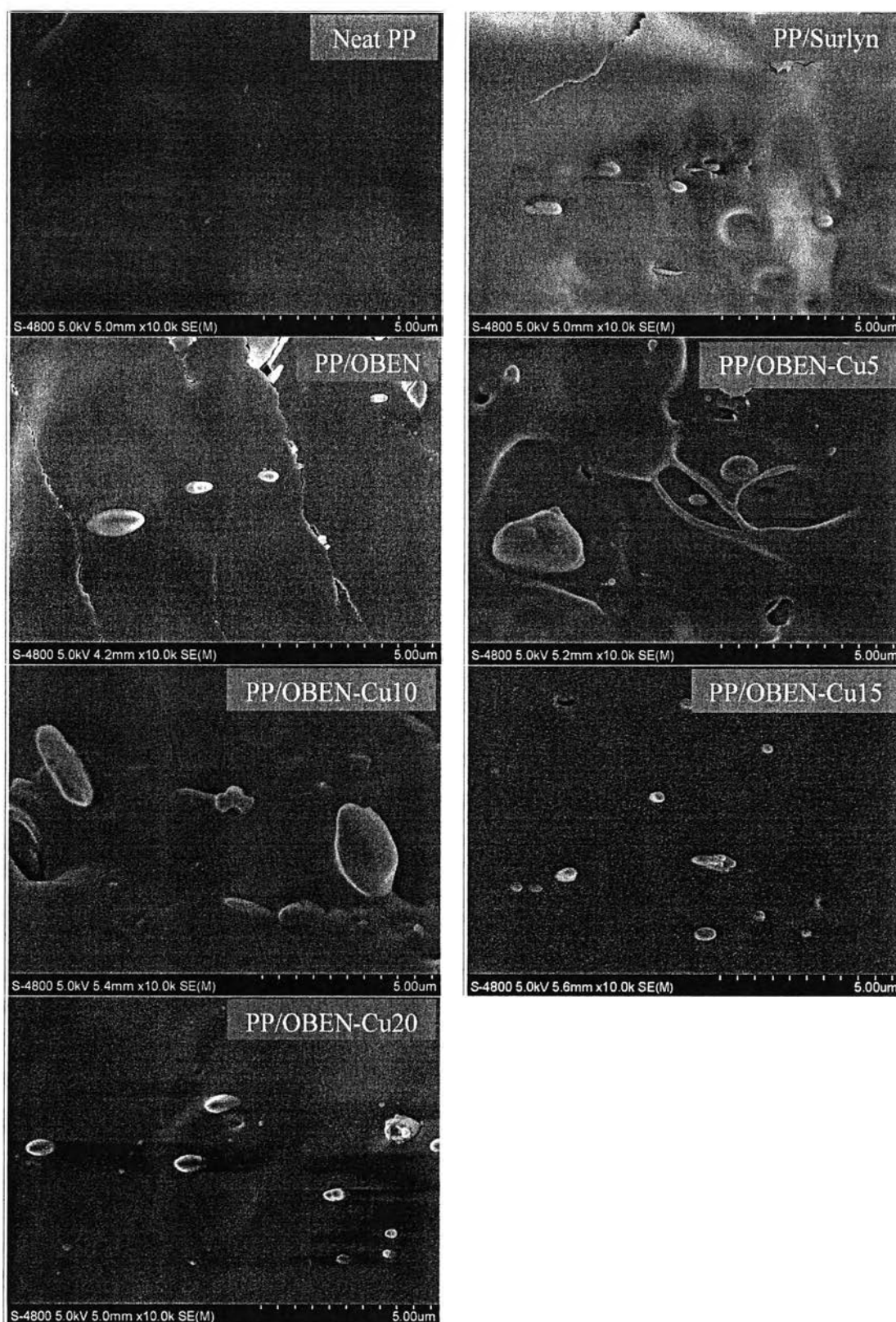


Figure 5.9 Cryo-fractured SEM micrographs of neat PP, PP/Surlyn and PP nanocomposite blown films (magnification 10,000X).

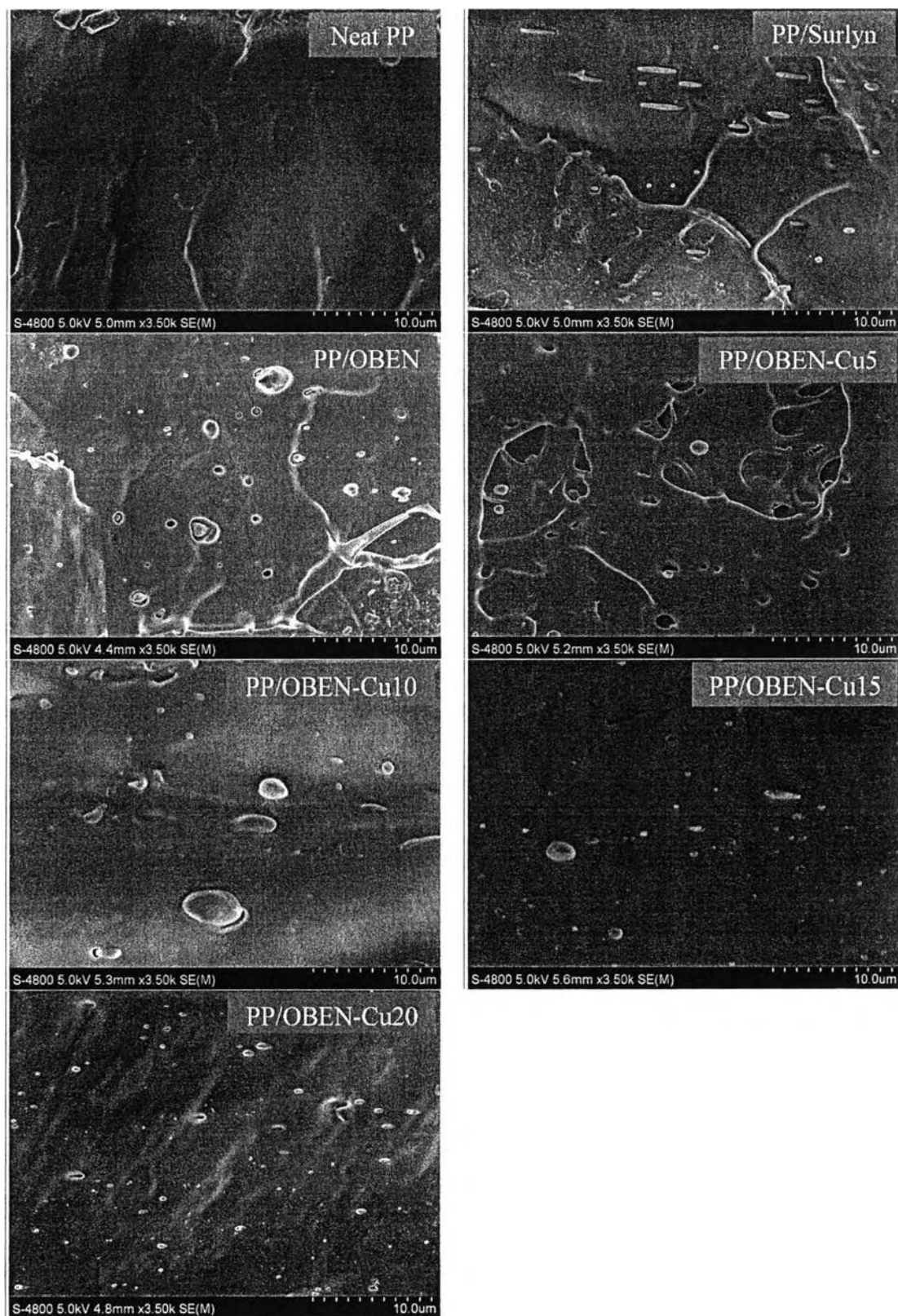


Figure 5.10 Cryo-fractured SEM micrographs of neat PP, PP/Surllyn and PP nanocomposite blown films (magnification 3,500X).

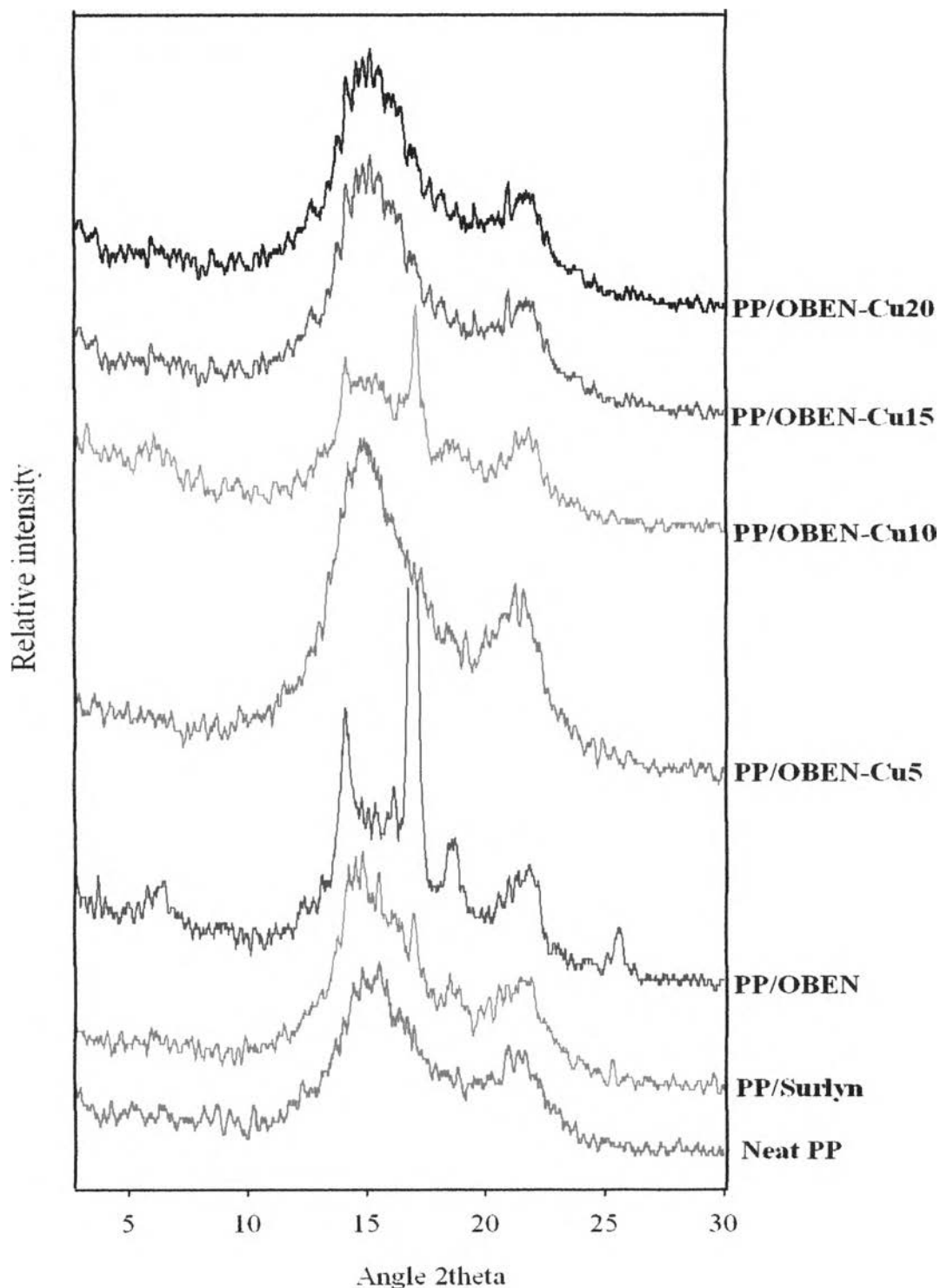


Figure 5.1 XRD patterns of neat PP and PP nanocomposite films showing crystals of PP matrix. The XRD patterns of each sample have a common scale such that any increase or decrease in intensity of particular peak is a direct measure of the percentage of crystallization.

Figure 5.11 shows the XRD patterns of neat PP, PP/Surlyn and PP/Surlyn/OBEN-CuNPX blown film samples from $2\theta = 2^{\circ}$ – 30° . Polypropylene (PP) is characterized by four different crystalline phases that which include monoclinic (α), hexagonal (β), orthorhombic (γ), and mesomorphic (smectic). The nucleation of these different polymorphs depends on the crystallization conditions. The commonly observed crystalline phase of polypropylene is α -phase (α -PP), which is characterized by six distinct peaks at 2θ values of ~ 14.2 , 17.0 , 18.7 , 21.3 , 21.7 and 25.4° , respectively. These peaks individually correspond to the (110), (040), (130), (111), (041) and (060) reflections. (Fages *et al.*, 2011, Yuan *et al.*, 2010). In this study, the neat PP blown film sample is characterized by two broad peaks at 2θ values of $\sim 15.5^{\circ}$ and 22.0° with low intensity indicating relatively low %Crystallinity in neat PP blown film fabricated by water-quenched blown film process. In DSC results, the %Crystallinity in the first heating scan is lower than those in the second heating scan for about 30-40%.

In PP/Surlyn films, almost the same XRD pattern is obtained. It is found the presence of the small peaks at $2\theta = 17.0^{\circ}$ corresponding to (300) reflection of β -phase. The presence of the β -phase is believed to be nucleated because of the nucleating effect by Surlyn dispersed phases. There have been reports that the β -phase (β -PP) nucleates in the presence of nucleating agent or under specific conditions of temperature gradient and strain. Occasionally, reinforcement minerals may act as β -nucleating agents. (Yuan *et al.*, 2010). Also, the increase in percentage of crystallinity of the blown film with the presence of Surlyn is also supported by DSC tests later.

In PP/Surlyn/OBEN blown films, the distinct peak at $2\theta = 17.0^{\circ}$ becomes outstanding from the XRD patterns indicating the β -phase of PP crystals are present in a certain amount. Also, the α -peaks are more distinct indicating more complete spherulites are formed. Some of the OBEN are exfoliated in the PP matrix (evident in the next XRD pattern) and act as the nucleating sites for PP molecules to nucleate and form spherulite in β -form. XRD patterns of PP/Surlyn/OBEN-CuNPx samples show the same XRD patterns with higher intensity compared to neat PP films, however, the peak of β -PP disappears in all the PP/OBEN-CuNPx

nanocomposite films except in the 10 wt% CuNP loading samples. This would attribute to better exfoliation of OBEN in the PP matrix with the presence of CuNP incorporating into OBEN particles.

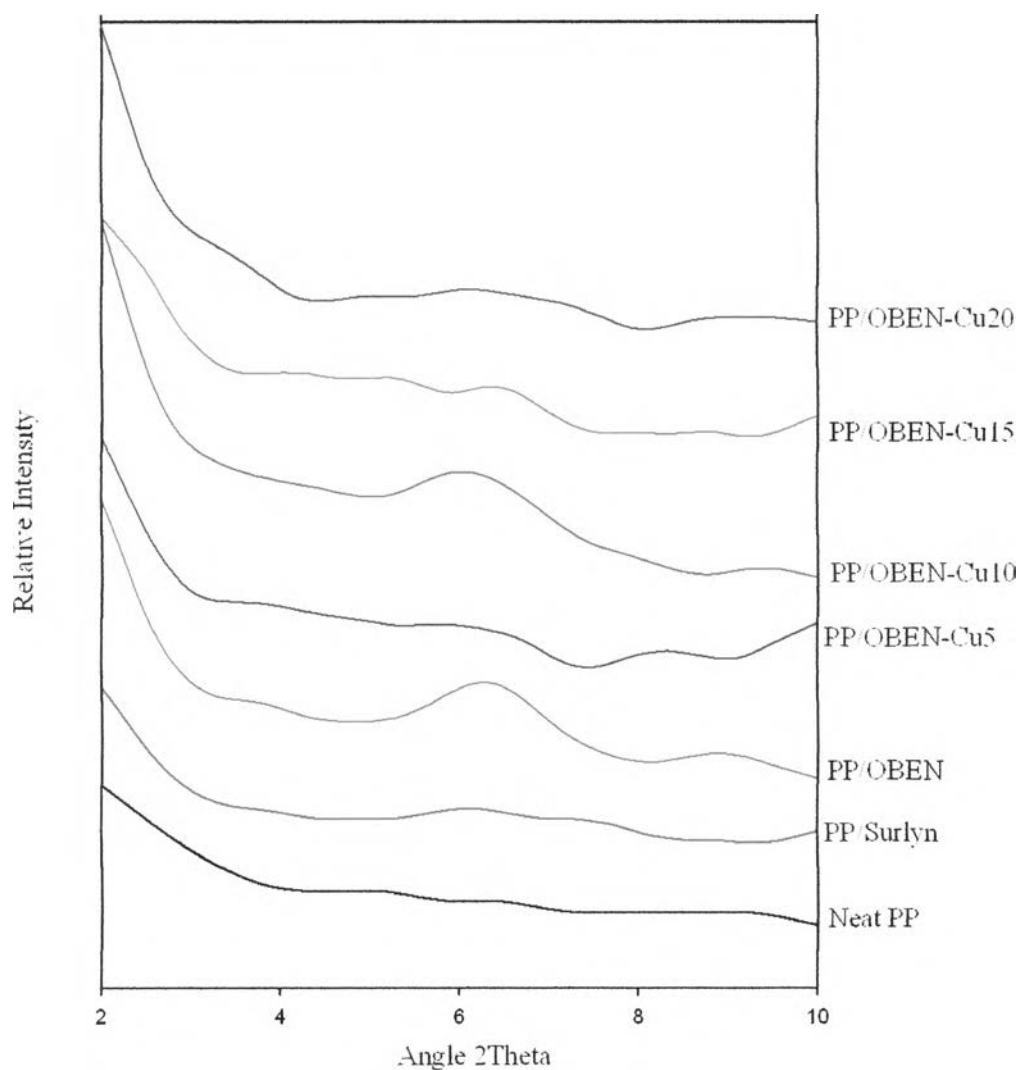


Figure 5.1 XRD patterns of neat PP and PP nanocomposite blown films showing intercalation and exfoliation of nanoclay in PP matrix.

Figure 5.12 the XRD patterns of neat PP, PP/Surlyn and PP/Surlyn/OBEN-CuNP_x blown film samples from $2\theta = 2^\circ - 10^\circ$. From Fig.44, the OBEN has the characteristic peaks at $2\theta = 5.67^\circ$ and 4.09° which corresponding to d-spacing of 1.56 and 2.15 nm, respectively. Compared to the XRD pattern in

PP/OBEN, the $2\theta = 4.09^\circ$ corresponding to d-spacing of 2.15 nm disappears. This refers to the breakage of silicate layers (or exfoliation) of nanoclay that having the organic ion intercalated inside the silicate layers. In PP/OBEN-CuNP films, the peak at 4.09° corresponding to d-spacing of 2.15 nm disappears similarly to the PP/OBEN sample, and the peak of the (001) basal diffraction of organoclay becomes more broadened and its intensity is weaker. As a result, the well-defined interlayer spacing is difficult to determine accurately. This result indicates that the stacks of layered silicates become more disordered, although a periodic distance is still maintained. Apparently, the partial exfoliation of the layered silicates could be responsible for the decrease in intensity (Lim *et al.*, 2010).

5.4.4 Thermal Properties of Neat PP and PP Nanocomposite Films

Melting temperatures of neat PP and PP nanocomposite blown films were studied by DSC technique. The thermal properties of films by the DSC technique are presented in Table 5.3, and their thermograms are graphically shown in Fig.5.13 and 5.14, respectively. It is worthy to note that the %Crystallinity (χ_c) in the 1st heating scan is less than those in the 2nd heating scan. This is due to the 1st heating scan indicates the thermal history of the blown films fabricated by water-quenched blown film process.

The 2nd heating scan would be used for the discussion in the role of nanoparticles in the thermal properties of PP film. It is found that crystalline melting temperature (T_m) of neat PP blown film was 159 °C with %Crystallinity of 43.40 in the 2nd heating scan. Adding Surlyn into PP matrix decreased T_m of PP; however, the percentage of crystallinity was increased from 43.40 to 45.65. This indicates that dispersed phases of ionic aggregates (Surlyn) acted as a nucleation sites for PP molecules to form crystallize. Meanwhile, they interrupted PP molecules to form larger spherulites causing T_m to be reduced. This observation is similarly to those reported by Lin *et al.* Also, this nucleating effect of Surlyn in PP crystallization is evident in the quenching process since the %Crystallinity in the 1st heating scan is 26.81% compared to 23.92% of neat PP.

Table 5.3 Thermal properties of neat PP and PP nanocomposite films

Abbreviations	T _{c,peak} (°C)	T _{m,peak} (°C) 1 st heating	T _{m,peak} (°C) 2 nd heating	% χ_c (1 st heating)	% χ_c (2 nd heating)
Neat PP	109.85	159.49	159.33	23.92	43.40
PP/Surllyn	109.86	158.89	156.05	26.81	45.65
PP/OBEN	109.06	160.25	156.98	30.09	43.30
PP/OBEN-Cu5	110.31	159.85	157.19	27.75	45.13
PP/OBEN-Cu10	111.41	160.38	156.24	26.45	44.59
PP/OBEN-Cu15	110.48	159.56	158.05	27.57	46.62
PP/OBEN-Cu20	109.86	160.56	158.21	27.08	47.86

Note: PP 100% crystallinity, $\Delta H_m^* = 209$ J/g

$$\text{For the 2}^{\text{nd}} \text{ heating, } \chi_c = \frac{\Delta H_m / \phi}{\Delta H_m^*} \times 100$$

where ΔH_m is the melting enthalpy of the PP sample, ΔH_m^* is the enthalpy for 100% crystalline PP, and ϕ is the mass ratio of PP in the PP nanocomposite sample.

$$\text{For the 1}^{\text{st}} \text{ heating, } \chi_c = \frac{(\Delta H_m - \Delta H_c) / \phi}{\Delta H_m^*} \times 100$$

where ΔH_m is the melting enthalpy of the PP sample, ΔH_c is the crystallization enthalpy of the PP sample during the heating scan, and ΔH_m^* is the enthalpy for 100% crystalline PP, and ϕ is the mass ratio of PP in the PP nanocomposite sample.

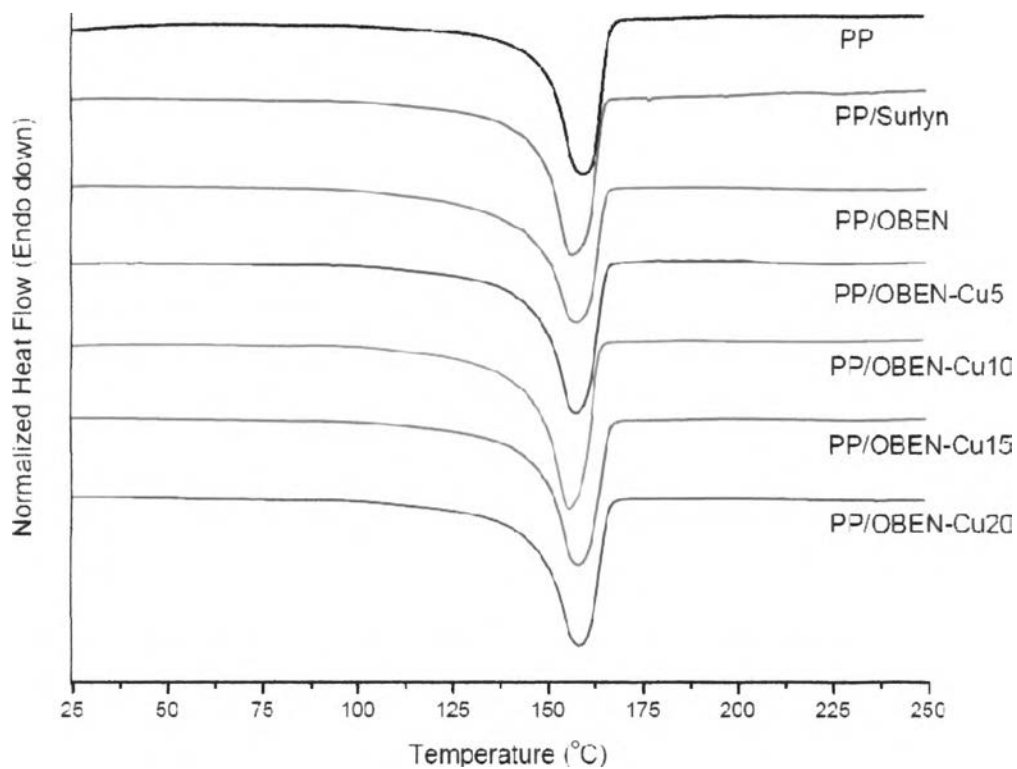


Figure 5.1 2nd heating scan of neat PP and PP nanocomposite films.

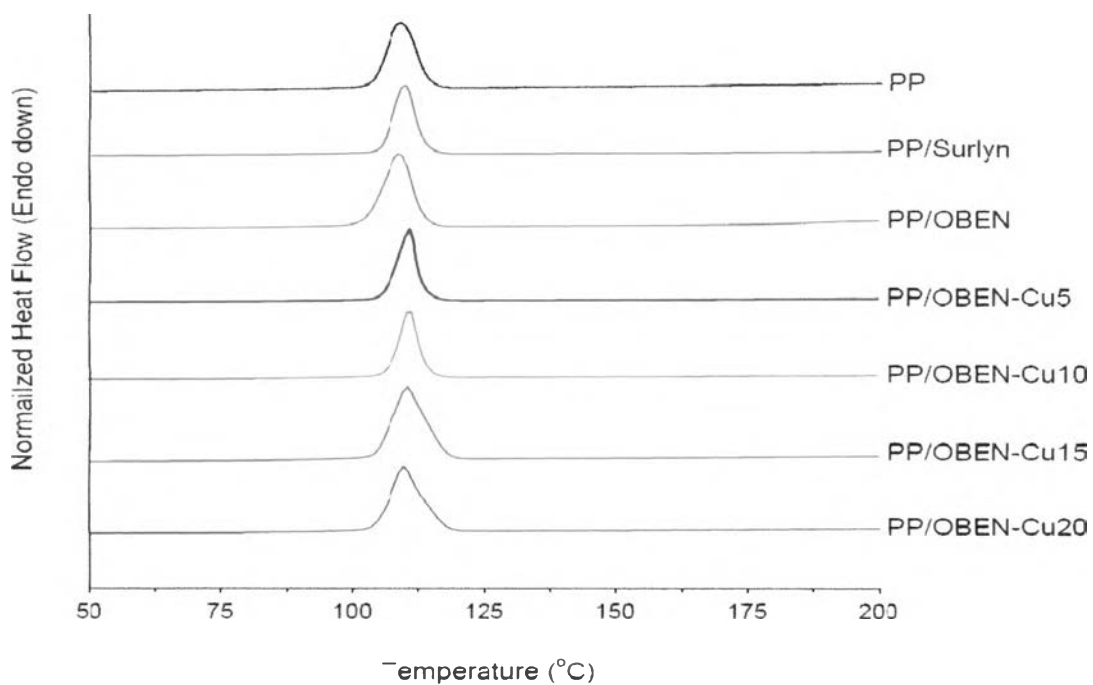


Figure 5.2 DSC cooling scans of neat PP and PP nanocomposite films.

Compared to neat PP, adding 1 wt% of OBEN with the presence of Surlyn decreased T_m of PP, but the %Crystallinity was in the same range for the 2nd heating scan. This indicates that the well-dispersion of organoclay in PP matrix inhibited PP molecules to form complete spherulites. Lim *et al.* reported a synergistic effect between Surlyn and clay in suppressing the accelerating crystallization on PP matrix. They argued that there was a strong charge interaction between clay platelets and ionic aggregates in Surlyn phase, which could weaken nucleating effect of ionic aggregates (Surlyn) on PP matrix. Furthermore, the clay platelets localized at the interface prevent the contact of Surlyn domains from PP matrix during crystallization. It should be noted that the %Crystallinity in the 1st heating scan is higher than neat PP and PP/Surlyn significantly. This is attributed to the combination of nucleating effect of OBEN-Surlyn and the molecular orientation of PP molecules during the bubble stretching to allow crystallization to form in higher degree.

For PP nanocomposite blown films adding OBEN-CuNP in various ratios, it is found that the crystalline melting temperatures (T_m) were slightly increased compared to PP/OBEN samples but still lower than those of neat PP. Nevertheless, the percentages of crystallinity were marginally higher with respect to CuNP contents. Also, the crystallization temperature (T_c) of PP/OBEN-CuNP samples appeared at higher temperatures than neat PP. This could be attributed to the nucleation effect of PVP-coated CuNP and the lesser content of OBEN dispersed in the PP matrix. As for the weight ratio of organoclay decreased, there was less clay particles to have interactions with Surlyn dispersed phases and hinder the mobility of polymer chains, resulting to increase of the spherulite growth along with the enhanced nucleating activity of Surlyn phases as nucleation sites. PP molecules could also nucleate the crystallization of PVP-coated CuNP that dispersed in the PP matrix.

Fig.5.14 presents thermal degradation thermograms of neat PP and PP nanocomposite blown films studied by TGA technique under nitrogen atmosphere. Table 5.4 summaries their initial (onset) degradation temperatures (T_i), final degradation temperatures (T_f), inflation degradation temperatures (T_d), and char residues. It is found that neat PP film had the degradation temperature (T_d) at 445.6 °C leaving char residue of 3.2 wt%. Adding Surlyn ionomer of 2 phr into PP

increased T_d to occur at 459.4 °C and left slightly higher char residue. It is reported that the ionic aggregates within ionomer could persist in the molten state up to 300 °C (Lim *et al.*, 2010), which is much higher than the melting temperature of PP. These aggregates thus delayed the onset degradation (T_i) of PP molecules to occur at somewhat higher temperature, but once the degradation of PP molecules occurred the rate of degradation was faster as evident in the slope of TGA curves.

Compared to PP/Surlyn sample, adding OBEN organoclay of 1 wt% into PP decreased T_d slightly but left higher char residue from the OBEN content (1 wt%). In all PP/OBEN-CuNP samples, the significant increase in T_d was observed compared to neat PP sample while their char residue was in the same range in PP/OBEN sample. The increase in T_d could attribute to the relatively high heat capacity of CuNP that could absorb much heat in the vicinity so that the PP molecules in those samples degraded at higher temperatures.

Table 5.4 TGA results of neat PP and PP nanocomposite blown films

Abbreviations	T_i (°C)	T_f (°C)	T_d (°C)	Char residue (wt%)
Neat PP	401.8	473.2	445.6	3.2
PP/Surlyn	430.7	485.2	459.4	4.1
PP/Surlyn/OBEN	428.3	484.4	458.7	5.1
PP/OBEN-Cu5	432.0	485.7	460.1	4.6
PP/OBEN-Cu10	432.1	486.5	460.7	5.1
PP/OBEN-Cu15	432.2	486.3	460.5	5.5
PP/OBEN-Cu20	431.3	486.6	460.0	5.4

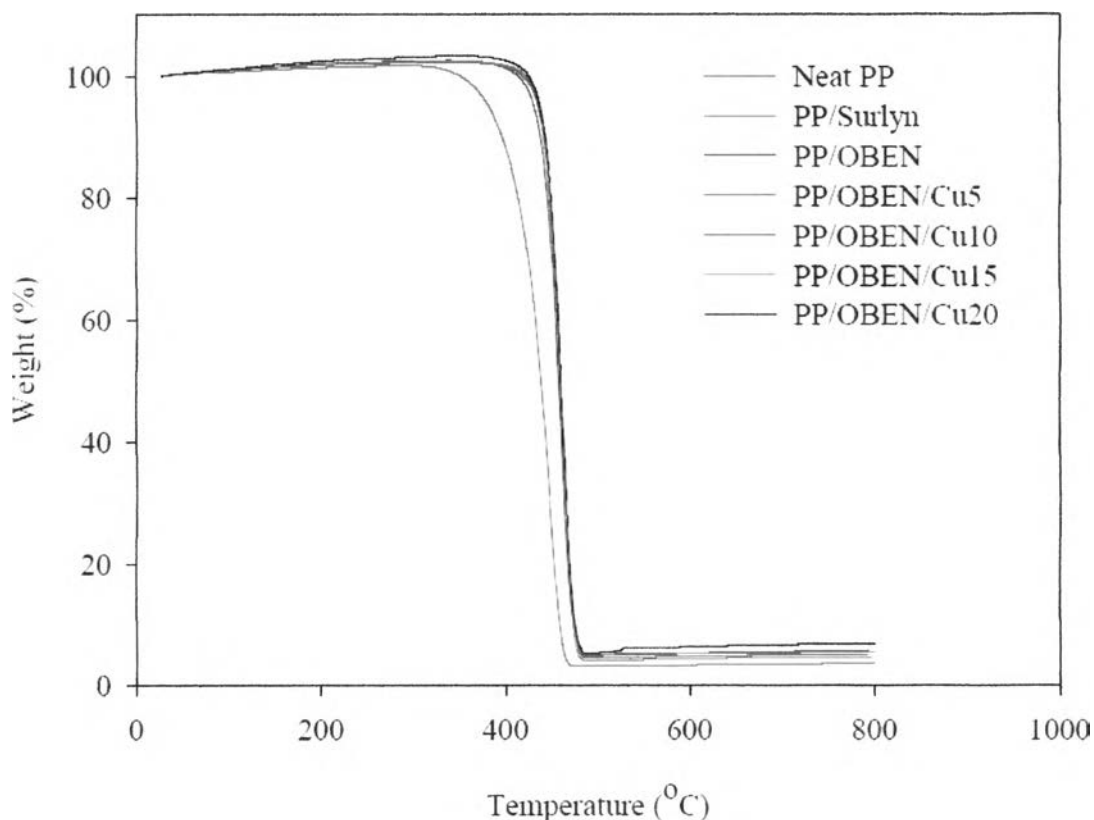


Figure 5.1 TGA thermogram of neat PP and PP nanocomposite blown films (under nitrogen atmosphere).

5.5 Conclusions

With the presence of OBEN-CuNP, PP nanocomposite blown films were haze and had higher yellowish tinge. Adding OBEN or OBEN-CuNP into PP films reduced the elongation at break of the films due to loss of film homogeneity. However, these nanocomposite films showed good elongation at break in machine direction over 300% compared to neat PP with elongation at break of 400%. Adding PVP-coated CuNP into PP films showed positive effect on tensile strength of nanocomposite films. This is due to Surlyn ionomer and nanoparticles acted as nucleating sites to increase crystallinity of PP nanocomposite films. Thermal stability of PP nanocomposite films was improved with the presence of nanoparticles. From the overall mechanical properties and clarity, it indicates that the PP nanocomposite

films would be capable to be used in prepacked chilled fish packaging since these films could be used to wrap around chilled fish with ease and could present the products properly.

5.6 References

- Chang, A.C. , Tau, L. , Hiltner, A. and Baer, E., (2002) Structure of blown film from blends of polyethylene and high melt strength polypropylene, Polymer, 43, 4923-4933.
- Fages, E. , Pascual, J. , Fenollar, O. , Garcí'a-Sanoguera, D. and Balart, R., (2011) Study of antibacterial properties of polypropylene filled with surfactant-coated silver nanoparticles, Polymer Engineering and Science, 51 (4), 804-811.
- Lim, H.T. , Liu, H. , Ahn, K.H. , Lee, S.J. and Hong, J.S., (2010) Effect of added ionomer on morphology and properties of PP/organoclay nanocomposites, Korean J. Chem. Eng. 27 (2), 705-715.
- Wu, C. , Mosher, B. and Zeng, T., (2006) One-step green route to narrowly dispersed copper nanocrystals, Journal of Nanoparticle Research, 8, 965–969.
- Yuan, Q. , Chen, J. , Yang, Y. and Misra, R.D.K., (2010) Nanoparticle interface driven microstructural evolution and crystalline phases of polypropylene: The effect of nanoclay content on structure and physical properties, Materials Science and Engineering A, 527, 6001-6011.
- Zhong, Y. and Kee, D.D., (2005) Morphology and properties of layered silicate-polyethylene nanocomposite blown films, Polymer Engineering and Science, 45 (4), 469-477.
- Zhong, Y. , Janes, D. , Zheng, Y. , Hetzer, M. and Kee, D.D., (2007) Mechanical and oxygen barrier properties of organoclay-polyethylene nanocomposite films, Polymer engineering and science, 1101-1107.